

Gain Scheduled LQ Optimal Control of a Parametric Light Commercial Helicopter Model at Sea Level

Erkan Abdulhamitbilal¹, Elbrous M. Jafarov² and Levent Güvenç³
ROTAM Centre
Istanbul Technical University
Aeronautics and Astronautics Faculty, 34469 Maslak, Istanbul
Türkiye.

Abstract: - In this study, linearized MIMO helicopter flight dynamics are calculated via the commercial software Flight-Lab. In the following step, parametric linearized flight dynamics are obtained via curve fitting of each matrix element for 0-120 kt forward speed range under sea level flight conditions. Then, an LQ optimal control law is designed as an adaptive controller with gain scheduling, which is widely used in the aerospace field. The controller stabilizes the system and eliminates any initial errors in approximately 15 seconds. Stability of the open-loop and closed-loop systems are checked by plotting the eigenvalues for the calculated speed range. For different initial conditions, the time responses of the states and control inputs are used to demonstrate the controller performance and closed-loop system behavior that are achieved. Linearized flight dynamics matrices with optimal gain for 40 kt (67.5 ft/s) forward speed at 90ft (sea level) are given. Parameterization of matrices, calculation of adaptive controller (gain scheduler) and simulations are done by using Matlab-Simulink programming.

Key-Words: - Adaptive control, gain scheduler, LQ optimal control, parametric modeling, helicopter dynamics,

1 Introduction

Helicopter dynamics performance and control techniques are studied widely in reference [1]. Helicopter aerodynamics and techniques such as inflow, rotating blade motion and airfoil blade element analysis are studied in [2] where the commercial software Flight-Lab is used. Optimal control theory is investigated in [3]. Aircraft linear modeling, simulation and control techniques are given in references [4] and [5]. Bailey rotor model is given and modeled in reference [6]. Peter/He inflow model is used in a simulation of helicopter shipboard lunch system in reference [7]. A nonlinear optimal control of helicopter by using fuzzy gain scheduling is studied in reference [8]. Helicopter control design by using feedback linearization is studied in reference [9].

In this study, linearized MIMO helicopter flight dynamics are calculated via the commercial software Flight-Lab. In the following step, parametric linearized flight dynamics are obtained via curve fitting of each matrix element for the 0-120 kt forward speed range under sea level flight. Then, an LQ optimal control law is designed as an adaptive controller with gain scheduling based on forward speed as is widely used in the aerospace field. The controller stabilizes the system and eliminates any initial errors in approximately in 15 seconds. Stability of the open-loop and closed-loop systems is checked by plotting the eigenvalues for the calculated speed range. For different initial conditions,

the time responses of the states and control inputs are used to show the controller performance and closed-loop system behavior. Linearized flight dynamics matrices with optimal gain for 40 kt (67.5ft/s) forward speed at 90 ft (sea level) are given. Parameterization of matrices, calculation of adaptive controller (gain scheduler) and simulations are presented.

The rest of the paper is organized as follows. Section 2 deals with the dynamics of a light commercial helicopter (LCH) and concentrates on linearized parametric models and stability analysis. LQ optimal control is presented in Section 3. Section 4 is on the parametric linear model and its use in obtaining the adaptive (gain scheduler) control algorithm. A simulation study is also presented in Section 4. The paper ends with conclusions given in the last section.

2 Helicopter Dynamics

A Flight-Lab model of the light commercial helicopter considered here was prepared and used in the linearization and stability analysis, forward velocity scheduled LQ optimal controller design and simulation studies in this paper. Some of the important features of this Flight-Lab light commercial helicopter model are briefly presented in this section.

In single rotor helicopters, the main rotor produces the leading lift force with side forces to move the airframe forward, sideways or upward. The main rotor hub is chosen to be articulated with linearly twisted flexible

blades connected to the hub with a flexure element and torque tubes. The inflow model of the main disc that calculates the induced velocity is modeled using the Peters/He finite state method which is set up with four inflow harmonics and eight higher powers of radial variation. The main rotor parameters such as dimensions, hub position, and nominal rotation speed used here are given in Table 1.

The tail rotor reacts to stabilize the side forces and torque produced by the drag force of the rotor blades. In other words, tail rotor produces anti torque for the main rotor and changes the heading angle of the helicopter according to pedal inputs. Tail rotor is modeled simply with the Bailey rotor model [6] with a linear lift curve slope in pusher mode with high blockage effects at low forward speeds. Table 1 also shows some parameters of the tail rotor that are used in modeling.

The horizontal stabilizer reduces the pitch angle of the airframe in forward flight for high pitching moments of fuselage and main rotor that correspond to improved flying qualities and longitudinal stability. In this design, the horizontal stabilizer is selected to be fixed in the downwash at hover and to exit the downwash approximately at 30 kt in forward flight. Moreover, symmetric airfoil data is used in Flight-Lab model as a look-up table for calculation of lift and drag forces. Some aerodynamic data like span and position of the horizontal stabilizer are given in Table 1.

The vertical fin improves the lateral aerodynamical stability in forward flight after 40 kt. However, at low forward speeds, the vertical fin blocks the tail rotor downwash, which results in a reduction of rotor power if the ratio of distance between the rotor and fin is not set properly according to the tail rotor radius. A non-symmetric airfoil data is used in Flight-Lab model as a look-up table for calculation of lift and drag forces here. Data used for the span and position of the vertical fin are also given in Table 1.

The fuselage is a structural part which should be taken into account during the helicopter design process for proper stiffness, flexibility and mode shapes. The fuselage also plays an important role in aerodynamics and rigid body dynamics. Aerodynamics effects such as drag, lift, and side forces; rolling, pitching, and yawing moments, with the moment of inertias and weight effects are important in simulation which are considered carefully in the Flight-Lab model. Some data like position of the center of gravity, the moments and the products of inertia and total mass of the vehicle are given in Table 1.

Flying controls are assumed to be mechanical with hydraulic support for a single pilot system. In this study, pilot reference inputs are neglected and the aim is to achieve stabilization of the rotorcraft in the 0-120 kt speed range to trim conditions at sea level. The

horizontal stabilizer is fixed and there is no yaw stability augmentation system. The designed LQ optimal controller is used to stabilize the longitudinal, lateral and coupled motions at the same time.

A helicopter has four control inputs which are illustrated in Fig.1. They are the longitudinal and lateral cyclic controls, the collective control and the pedal control. The first three control inputs change main rotor swash plate angles and vertical position whereas the last control input changes tail rotor swash plate angle. Mechanical limits for the control system are assumed as follows. Swash-plate has pitching capability of ± 8 degrees for cyclic input and ± 8 for collective input which means totally 32 degrees of blade motion in pitching (downward pitch motion: $-8-8=-16$, upward pitch motion: $+8+8=+16$). The change of angle of attack of the tail rotor is between $-10/+15$ degrees, totally 25 degrees tail rotor pitching, for the selected tail rotor blade airfoil profile for pedal inputs.

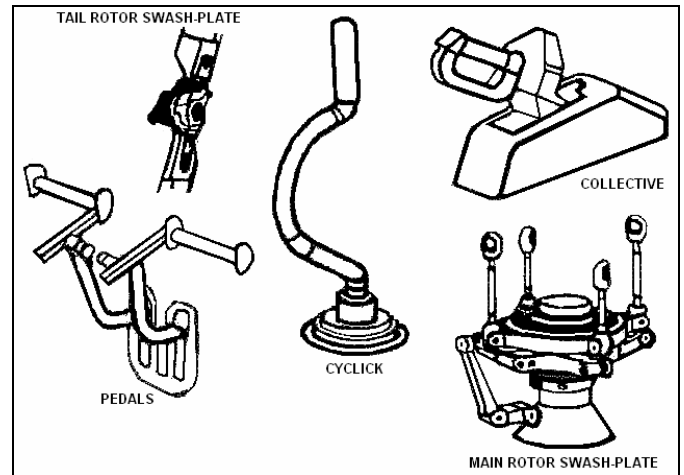


Fig.1 Control system elements: cyclic, collective, pedals, swash-plates of main and tail rotors.

In this study, helicopter modeling, aerodynamics, rigid-body dynamics, simulations, trim and linearization are studied with a commercial software Flight-Lab as mentioned above. So, the linearization outputs like system and control distribution matrices, trim outputs like attitude angles are used as an initial point for designed parametric helicopter flight dynamics and linear quadratic optimal controller. The linearized flight dynamics of a helicopter are treated in the next sub section.

2.1 Linearized helicopter flight dynamics

The linearized flight dynamics of the helicopter can be written as follows:

$$\dot{x} = Fx + Gu \tag{1}$$

where $x = [\phi \ \theta \ u \ v \ w \ p \ q \ r]^T$ are the states: roll angle, pitch angle, longitudinal speed, lateral speed, vertical speed, roll rate, pitch rate and yaw rate, respectively.

Also the control vector comprises lateral cyclic, longitudinal cyclic, collective and pedal inputs as $u = [X_a \ X_e \ X_c \ X_p]^T$, respectively. The system matrix F is (8×8) -dimensional and the input coupling matrix G is (8×4) -dimensional.

The output of the trim procedure of Flight-Lab gives the control inputs, the attitudes and speeds of the helicopter. On the other hand, linearization procedure gives the system matrix F and the control distribution matrix G . Once the matrices for 0-120 kt speed range are obtained curve fit can be performed. So, each element of system and control distribution matrices can be obtained, respectively, according to forward speed u as shown below:

$$F_{ij} = f_k(u) = f_n u^n + f_{n-1} u^{n-1} + \dots + f_0 \quad (2)$$

$$G_{jk} = g_m(u) = g_n u^n + g_{n-1} u^{n-1} + \dots + g_0 \quad (3)$$

where f_k and g_k are fifth-degree polynomials obtained via curve fitting of each element of the system and control distribution matrices. f_n and g_n are polynomial coefficients. Each element of the system and control distribution matrices for the 0-120 kt speed range and the fitted polynomials are shown as dot and line, respectively, in Fig.5. Some polynomials of elements of F and G are given as below:

$$F_{3,2} = f_{18}(u) = -7.418 \times 10^{-12} u^5 + 3.6729 \times 10^{-9} u^4 \\ - 5.3307 \times 10^{-7} u^3 + 2.4257 \times 10^{-5} u^2 - 0.00051234u \\ - 32.151$$

$$F_{4,8} = f_{32}(u) = -1.0849 \times 10^{-11} u^5 + 8.3174 \times 10^{-9} u^4 \\ - 1.783 \times 10^{-6} u^3 + 0.0001562u^2 - 0.99664u \\ + 0.22863$$

$$F_{5,8} = f_{40}(u) = 2.6336 \times 10^{-11} u^5 - 1.7242 \times 10^{-8} u^4 \\ + 4.5405 \times 10^{-6} u^3 - 0.0005637u^2 + 0.031379u \\ + 1.2688$$

$$G_{3,2} = g_{10}(u) = -4.811 \times 10^{-12} u^5 + 3.2553 \times 10^{-9} u^4 \\ - 7.4482 \times 10^{-7} u^3 + 7.1886 \times 10^{-5} u^2 - 0.003269u \\ + 0.059448$$

$$G_{5,2} = g_{18}(u) = 1.2225 \times 10^{-12} u^5 + 8.5254 \times 10^{-10} u^4 \\ - 6.6207 \times 10^{-7} u^3 + 9.6683 \times 10^{-5} u^2 - 0.0011076u \\ + 0.042207$$

$$G_{8,4} = g_{32}(u) = 4.3377 \times 10^{-13} u^5 - 1.1073 \times 10^{-10} u^4 \\ - 7.9707 \times 10^{-9} u^3 + 2.9821 \times 10^{-6} u^2 - 8.7886 \times 10^{-5} u \\ + 0.00014259$$

In the same manner 64 items of $f_k(u)$ -functions for system matrix F , and 32 items of $g_k(u)$ -functions for control distribution matrix G are calculated for the linearized parametric flight dynamics.

2.2 Stability analysis of the linearized system

The stability of the MIMO system can be determined by calculation of the eigenvalues $\lambda_1, \lambda_2, \dots, \lambda_8$ of system

matrix F of the parametric linear model. The plot of the eigenvalues of linearized flight dynamics for 0-120 kt forward flight velocity with 10 kt steps at sea level are shown in Fig.2.

It can be seen that both lateral and longitudinal motions are unstable. Longitudinal instability occurs in phugoid eigenvalues which have positive real numbers but the short period eigenvalues are at the left side of s-plane with negative signs. Beside, lateral instability appears in dutch-roll eigenvalues in some forward speeds, but spiral mode has a negative signed eigenvalues for the 0-120 kt speed range.

As seen from the Fig.4 for the uncontrolled system, spiral mode has high frequencies such as $\omega_n = 6.7 - 10.44$ rad/s with $\xi = 0.3 - 0.5$ damping ratio for near hover motion. After 10 kt natural frequencies of spiral mode appears to be $\omega_n = 1.8 - 4.7$ rad/s and damping ratio becomes $\xi = 1$. At that point the spiral mode behaves normally. Dutch-roll effects are highly damped but natural frequencies have low values which corresponds to long settling time. On the other hand, short period motion has long settling time with damping ratio near $\xi = 0.33$. Phugoid motion is unstable for the whole speed range.

The results illustrate the stability picture of the rotorcraft clearly as: 1) It can be said that near hover motion some oscillations occurs in lateral dynamics because of spiral mode. 2) In dutch-roll mode in forward flight lateral dynamics response is stable with very long settling times. 3) Again in forward flight the change of pitch angle and pitch rate of the rotorcraft occur slowly because of the short period mode. And finally 4) In forward flight the rotorcraft can not keep the flight altitude because of the unstable phugoid mode. Note that, unstable phugoid eigenvalues affect the system quickly at high values of the forward speed.

3 LQ Optimal Controller Design

Consider the plant described with linearized flight dynamics equation (1). The performance measure to be minimized is

$$J = \frac{1}{2} \int_0^{\infty} (x^T Q x + u^T R u) dt \quad (4)$$

where Q is a real symmetric positive semi-definite matrix, R is a real symmetric positive definite matrix, x and u are states and control vectors, respectively. In the design process, it is assumed that the states and controls are not bounded. However, control inputs are bounded due to physical limitation of the swash plate mechanism and also states of the system are bounded because of aerodynamics rules and performance of power-plant. So, the aim is to maintain the state vector close to the origin without an excessive expenditure of control effort. Then, the Hamiltonian for (1) and (4) can be written as [3]:

$$H = \frac{1}{2}x^T Qx + \frac{1}{2}u^T Ru + \lambda^T Fx + \lambda^T Gu \quad (5)$$

and necessary conditions for optimality are [3]:

$$\dot{x}^* = Fx^* + Gu^* \quad (6)$$

$$\dot{\lambda}^* = -\frac{\partial H}{\partial x} = -Qx^* - F^T \lambda^* \quad (7)$$

$$0 = \frac{\partial H}{\partial u} = Ru^* - G^T \lambda^* \quad (8)$$

Form (6), the optimal control law is obtained as:

$$u^* = -R^{-1}G^T \lambda^* \quad (9)$$

Substituting the optimal control law (9) into (6) results 2n linear homogenous differential equations whose solution is:

$$\lambda^* \triangleq Kx^* \quad (10)$$

which means that λ^* is a linear function of states of the linear system and K is the (8x8)-dimensional symmetric matrix. Also K is the solution of following Algebraic Riccati Equation (ARE):

$$F^T K + KF + Q - KGR^{-1}G^T K = 0 \quad (11)$$

Substituting (10) into control law (9) the optimal control law or Kalman gain becomes

$$u^* = -R^{-1}G^T Kx^* \triangleq Cx^* \quad (12)$$

which indicates that the optimal control law is linear and a combination of the system states.

Finally, the optimal cost of performance index can be calculated from:

$$J = \frac{1}{2}x^T(0)Kx(0) \quad (13)$$

Therefore, an optimal control law is designed for the linearized flight dynamics of the LCH at sea level.

4 Parametric Linear Helicopter Modeling and Computer Simulations

The flight dynamics of LCH are modeled parametrically according to 0-120 kt forward speed range in Section 2. A control law is designed for stabilization of the helicopter with LQ optimal control techniques in Section 3. In this work, because of parametric helicopter flight dynamics, control law has to be adaptive for any change of helicopter dynamics (but mainly based on forward speed). In the next subsection adaptive LQ optimal control algorithm (gain scheduler) is proposed.

4.1 Parametric linear helicopter modeling with adaptive closed-loop for 0-120 kt speed range at sea level

The closed-loop flight dynamics equation of the helicopter for 0-120kt forward speed range can be written from (1) and (12) as follows:

$$\dot{x} = [F - GC]x = [F - GR^{-1}G^T K]x \quad (14)$$

where F and G are parametric matrices which depend on the forward speed defined via (2) and (3).

The control law in this manner is LQ optimal and the Kalman gain C is calculated at any step of simulation during the changes of the forward speed. In other words, the gain matrix C is scheduled for any forward speed u , and that is why the control law is adaptive. The Matlab code for calculation of the control law is given in Table 2. The weighting matrices Q and R are selected to be for the speed range of 0-120 kt as below.

$$Q = \text{diag}(0,0,3,3,3,0.5,0.5,0.5) \quad (15)$$

$$R = \text{diag}(0.8,0.8,0.8,0.8) \quad (16)$$

The cost of performance index for selected LQ optimal controller of 0-120 kt speed range with six different initial conditions are calculated and displayed in Fig.2. The y-axis of the plot is shown in logarithmic scale to make a visual relation between the costs of performance index for the different initial conditions. The initial conditions are assumed to be as:

Case 1: $r=0.1,0.2,0.3\text{rad/s}$; $u,v,w=0\text{ft/s}$, $p,q=0\text{rad/s}$

Case 2: $q=0.1,0.2,0.3\text{rad/s}$; $u,v,w=0\text{ft/s}$, $p,r=0\text{rad/s}$

Case 3: $p=0.1,0.2,0.3\text{rad/s}$; $u,v,w=0\text{ft/s}$, $q,r=0\text{rad/s}$

Case 4: $w=2,4,6,8\text{ft/s}$; $u,v=0\text{ft/s}$, $p,q,r=0\text{rad/s}$

Case 5: $u=2,4,6,8\text{ft/s}$; $v,w=0\text{ft/s}$, $p,q,r=0\text{rad/s}$

Case 6: $v=2,4,6,8\text{ft/s}$; $u,w=0\text{ft/s}$, $p,q,r=0\text{rad/s}$

Longitudinal stabilization for initial conditions specified by Case 2, 4 and 5 according to costs of performance index (13) seems to be expensive while forward speed increases in x-axes. Note that, vertical speed w and pitch rate q have quite the same trends and high costs of performance index as seen from the figure. As a result, it can be said that longitudinal stabilization requires more control effort.

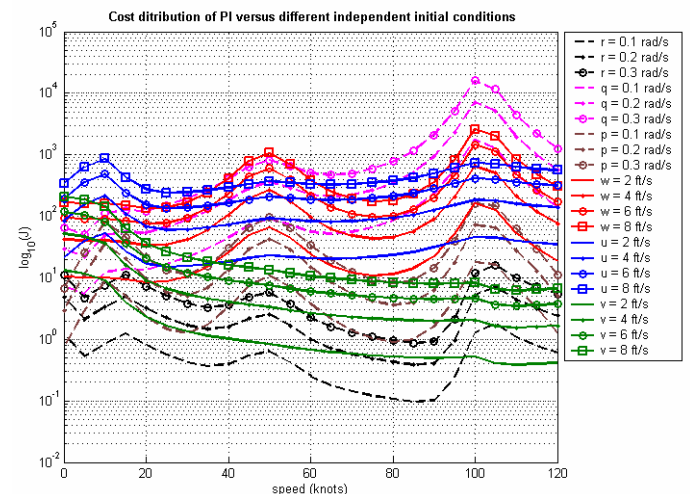


Fig.2 Cost variation for 0-120kt of three different initial conditions

Lateral stabilization for initial conditions specified by Case 1, 3 and 6 according to costs of performance index (13) seems to be cheap while forward speed increases in

the x-axis. To eliminate any initial errors for sideways velocity v is very easy and less control inputs are required. On the other hand, yaw rate r and roll rate p have the same trends as w and q but with less cost values. Finally, it can be said that lateral stabilization requires less control effort than longitudinal one.

4.2 Stability analysis of closed-loop system

The stability of the MIMO system can be determined by calculation of the eigenvalues $\lambda_1, \lambda_2, \dots, \lambda_8$ of the closed-loop system matrix $F - GR^{-1}G^TK$ (or $F - GC$) according to the optimal control law (12). As an example F, G, C matrices for 40 kt (67.5 ft/s) forward speed at 90 ft (sea level) are given in Table 3.

It can be seen that both lateral and longitudinal motions of closed-loop system are stable. However, short period of longitudinal motion has high frequencies for high forward speeds as shown in Fig.4. The LQ optimal controller pushes the short period eigenvalues more to the left of the s-plane. To obtain such a motion, an actuator with a good quality has to be used which is a must in aerospace engineering.

As seen from the Fig.4 for closed-loop system, spiral mode has high frequencies such as $\omega_n = 6.7 - 10.44$ rad/s with $\xi = 0.3 - 0.5$ damping ratio for near hover motion. After 10 kt natural frequencies of spiral mode appears to be $\omega_n = 1.8 - 4.7$ rad/s and damping ratio becomes $\xi = 1$ as same in open-loop system. At that point spiral mode behaves normally. Dutch-roll effects are highly damped but natural frequencies have low values which corresponds to long settling time. On the other hand, short period mode natural frequencies arise parallel with forward speed because of the weighting matrices of the LQ optimal controller and reaches $\omega_n = 17$ rad/s with approximately $\xi = 0.5$ damping ratio. Phugoid mode is stabilized with LQ optimal method and have natural frequencies range of $\omega_n = 0.01 - 1$ rad/s.

The results illustrate the stability picture of the closed-loop system clearly as: 1) It can be said that near hover motion some oscillations still occurs in lateral dynamics because of spiral mode. 2) In dutch-roll mode in forward flight lateral dynamics responses are stable with very long settling times. 3) Again in forward flight the change of pitch angle and pitch rate of the rotorcraft become fast because of the short period mode which has high natural frequencies. And finally, 4) The rotorcraft is stabilized to keep the flight altitude during forward flight.

4.3 Computer simulations

Block diagram of adaptive parametric LQ optimal control helicopter system is shown in Fig.3. Matlab-Simulink simulation results are illustrated in Fig.6,7 and 8 for different initial flight conditions and initial state errors. From the computer simulation easily it can be seen that the helicopter is stabilized by the gain scheduled LQ optimal controller at any forward speed of

0-120 kt approximately in 15 seconds. This settling time may be very long for such an optimal control system; however, considered design of LCH has some no-good configuration which need to be eliminated and corrected. In general, lateral dynamics are seemed to be sufficient to be easily controlled, but longitudinal dynamics need more control efforts for stabilization of helicopter.

5 Conclusion

In this study, linearized MIMO helicopter flight dynamics were calculated using the commercial software Flight-Lab. Parametric linearized flight dynamics were obtained via curve fitting for each matrix element for 0-120 kt forward speed range at sea level flight. An LQ optimal control law was designed as an adaptive controller with forward velocity based gain scheduling technique widely used. The controller stabilizes the system and eliminates any initial errors in approximately 15 seconds. Also stability of open-loop and closed-loop the systems are checked by plotting the eigenvalues for the calculated speed range. For different initial conditions the time responses of the states and control inputs are illustrated which show the controller performance and closed-loop system behavior. Linearized flight dynamics matrices with optimal gain for 40 kt (67.5ft/s) forward speed at 90ft (sea level) are given. Parameterization of matrices, calculation of adaptive controller and simulations are done by using Matlab-Simulink programming.

Note that, in the linear model, control law can be limited with a saturation function to illustrate the boundary of the control mechanism. Moreover, pedal inputs in hover and collective with longitudinal cyclic in maximum speeds in forward flights are used near %100. In these extreme cases, the bounds of control mechanism get an important point that designers have to be careful.

Using eigenstructure assignment method also is possible to select such a feedback gain. Unfortunately, setting the eigenvalues to a desired place may require high control inputs which are limited mechanically with main rotor swash-plate or collective input that changes rotor blade pitch angle and pedal inputs that change tail rotor pitch angle. This high gain may be applied mathematically in design procedure, however physically control inputs are mechanically and aerodynamically limited to produce always possible required lift forces and limited not to exceed the stall limits for rotor discs. Somehow exceeding limits of control mechanism may not guarantee the stability and the control of the rotorcraft.

For this manner LQ optimal method is applied with proper weighting matrices to stabilize the LCH with possible small optimal control inputs. The settling time may be thought that is very long, but for such a non-good design of LCH, stabilization is a problem when the system itself does not help to behave decisive to control

oscillations' frequency and damping of the motion done during the flight. So, the results of simulations show stabilizations of LCH with LQ optimal techniques.

Acknowledgement

This work is supported by the Istanbul Technical University's National Planning Association (DPT) funded HAGU Project Rotorcraft Research and Development Centre. Special thanks are extended to the directors Prof. Dr. H. Temel Belek, Prof. Dr. A. Rüstem Aslan and Flight-Lab modeling engineer F. Ersel Ölçer.

References:

[1] Raymond W. Prouty, *Helicopter Performance, Stability, and Control*, Krieger Publishing Company, Florida, 1995.
 [2] J. Gordon Lishman, *Principle of Helicopter Aerodynamics*, Cambridge University Press, New York, 2006,
 [3] Donald E. Kirk, *Optimal Control Theory*, Prentice Hall, New Jersey, 1970.
 [4] Brian L. Stevens and Frank Lewis, *Aircraft Control and Simulation*, John Wiley & Sons Inc ,1992
 [5] Donald McLean, *Automatic Flight Control Systems*, Prentice Hall, UK, 1990
 [6] F.J. Bailey, A simplified theoretical model of determining the characteristics of a lifting rotor in forward flight, NACA rep. no 716.
 [7] Dooyong Lee; Nilay Sezer-Uzol; Joseph F. Horn; Lyle N. Long, Simulation of Helicopter Shipboard Launch and Recovery with Time-Accurate Airwakes, *Journal of Aircraft*, vol. 42 no. 2, pp. 448-461.
 [8] Gwo-Ruey Yu, Nonlinear Optimal Control of Helicopter Using Fuzzy Gain Scheduling, *Proceedings of 2005 IEEE International Conference on Systems, Man and Cybernetics*, vol 4, pp. 3313-3318.
 [9] E. Liceaga-Castro R. Bradley and R. Castro-Linares, Helicopter control design using feedback linearization techniques, *Proceedings of the 28th Conference on Decision and Control*, Tampa, Florida December 1989

Table 1 Some design parameters of LCH

MAIN ROTOR	
Rotor direction	= Counterclockwise rotor
Rotor hub location	= 10.475722 0 5.583368 ft
Number of rotor blades	= 4
Blade tip loss factor	= 0.97
Hub orientation in Euler angles	= 0.0 177.0 0.0 deg
Rotor nominal speed	= 33.33 rad/sec
Rotor radius	= 18.0 ft
Articulated Blade model	= Flexible blade
Torque offset	= 0.0656168 ft
Rotor precone	= 0.061 rad
Flap hinge offset	= 1.564 ft
Feathering hinge offset	= 3.1662 ft
TAIL ROTOR	
Rotor hub location	= 31.505922 -0.65617 3.11526 ft
Number of rotor blades	= 4
Rotor radius	= 2.6 ft
Blade tip loss factor	= 0.92
Lift curve slope	= 5.73
Solidity weighted blade chord	= 0.52 ft
Tangent of delta three	= 0
Blockage effect for low speed	= 0.83
Speed threshold for blockage effect	= 30 knots
Rotor nominal speed	= 250.000 rad/sec
HORIZONTAL STABILIZER	
Lifting surface attachment point	= 26.849 ±0.72 2.301789 ft
Lifting surface sweep angle	= 0 deg
Lifting surface span	= 2.7048 ft
Initial incidence	= 0 deg
Lifting deficiency factor	= 0.6618
VERTICAL FIN	
Lifting surface attachment point	= 31.039370 -0.630906 3.15263 ft
Lifting surface sweep angle	= 30 deg
Initial incidence	= 7.2 deg
Lifting deficiency factor	= 0.6020
FUSELAGE	
Vehicle c.g.	= 10.789206 0 0.834421 ft
Total vehicle mass	= 4500.0 lbm
Total roll moment of inertia	= 1907.3 slug-ft ²
Total pitch moment of inertia	= 4231.4 slug-ft ²
Total yaw moment of inertia	= 3409.0 slug-ft ²
Total X-Y product of inertia	= -5.42 slug-ft ²
Total X-Z product of inertia	= 396.1 slug-ft ²
Total X-Y product of inertia	= 0.0332 slug-ft ²

Table 2 Matlab code for calculation of Kalman gain

```
S = 0*eye(8,4);
E = eye(8);
[P,L,G,RR] = care(A,B,Q,R,S,E);
C = R*(B')*P;
```

Table 3 Linearized flight dynamics matrices with optimal gain for 40kt (67.5ft/s) forward speed at 90ft (sea level)

A =	0	-0.0001	0	0	0	1.0000	-0.0009	0.0395	B =	0	0	0	0
	0.0001	0	0	0	0	0	0.9998	0.0217		0	0	0	0
	0.0106	-32.1709	-0.0225	0.0920	0.0160	-0.3899	0.2551	-0.1524		0.1318	0	0.0057	0.0057
	32.1625	0.0367	0.0125	-0.1561	0.0194	0.7355	-1.2002	-66.7339		0.1261	0.0630	0	0
	0.7207	-1.1941	-0.0888	-0.0193	-0.6556	3.7325	67.9414	1.8976		-0.3839	-0.3266	0.0802	-0.0172
	-0.0012	0.0030	0.0051	-0.0579	0.0554	-3.5970	-1.8338	0.2260		0.3094	0.0458	0.0172	-0.0057
	-0.0025	-0.0007	0.0085	-0.0113	0.0119	-0.2316	-2.3280	-0.0038		-0.0229	0	0	0
	-0.0026	0.0039	-0.0168	0.0234	-0.0227	0.2162	0.3670	-0.8710		-0.7334	-0.0286	-0.0516	0.0115
C =	0.7745	-92.5125	0.9224	0.6927	-0.4441	1.4142	-42.6209	-6.4394					
	-0.0633	-10.5789	-0.1652	0.0344	-0.5576	0.5816	-17.0387	0.4487					
	0.6199	10.5560	0.0379	0.0447	0.2321	-0.3020	9.5471	-0.9773					
	-0.2572	-2.5541	0.0385	-0.0096	-0.0493	0.0060	-1.8759	0.1863					

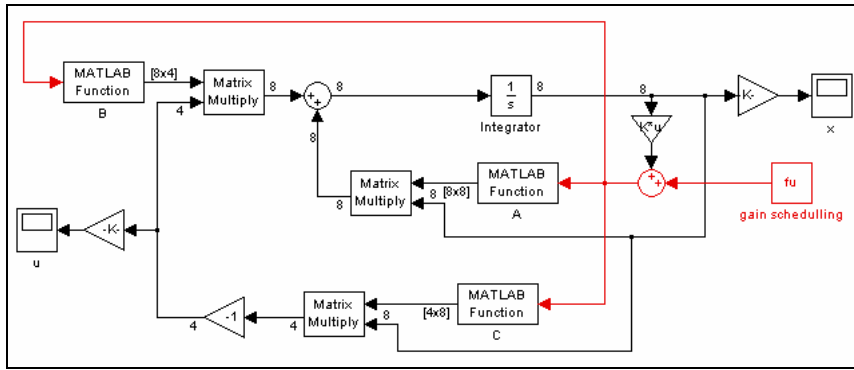


Fig. 3 Block diagram of adaptive parametric LQ optimal system

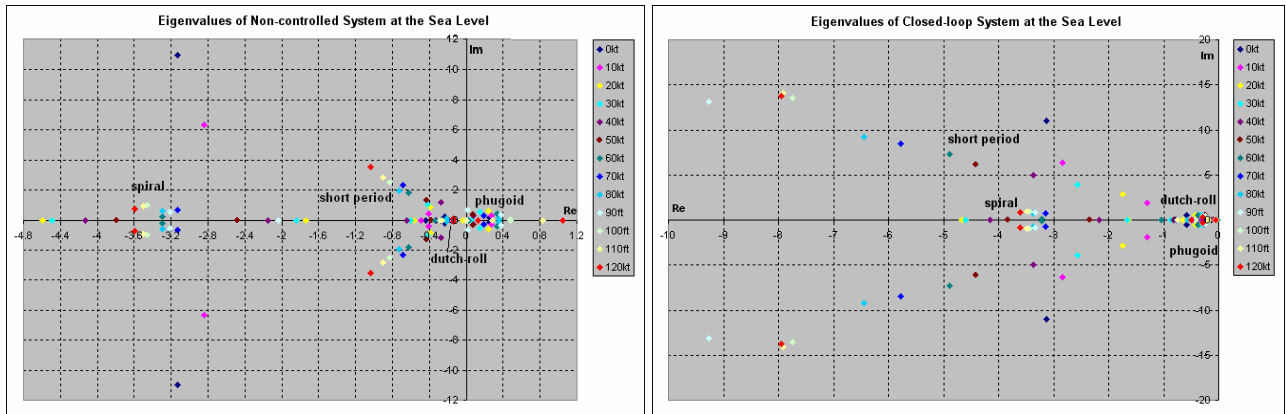


Fig.4 Eigenvalue plot of non-controlled and closed-loop system at the sea level

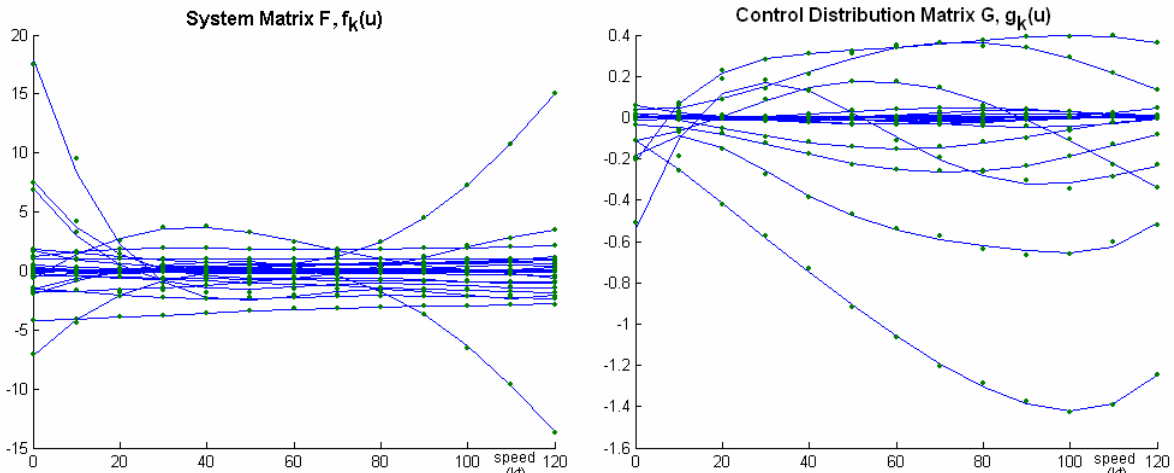


Fig.5 Curve fit for system matrix F ($f_{18}(u), f_{25}(u), f_{32}(u), f_{39}(u)$ are not included) and control distribution matrix G .

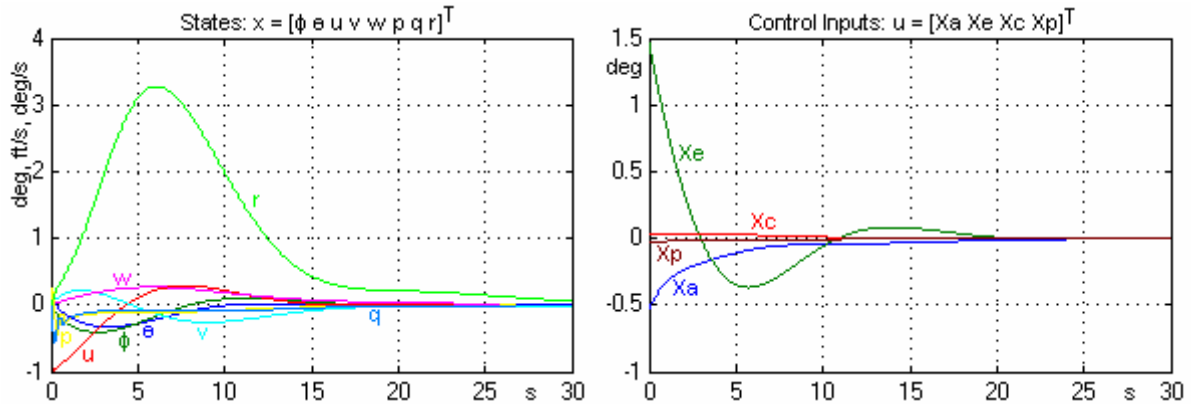


Fig.6 Time responses of states and control inputs in hover at the sea level ($u = -1ft/s$)

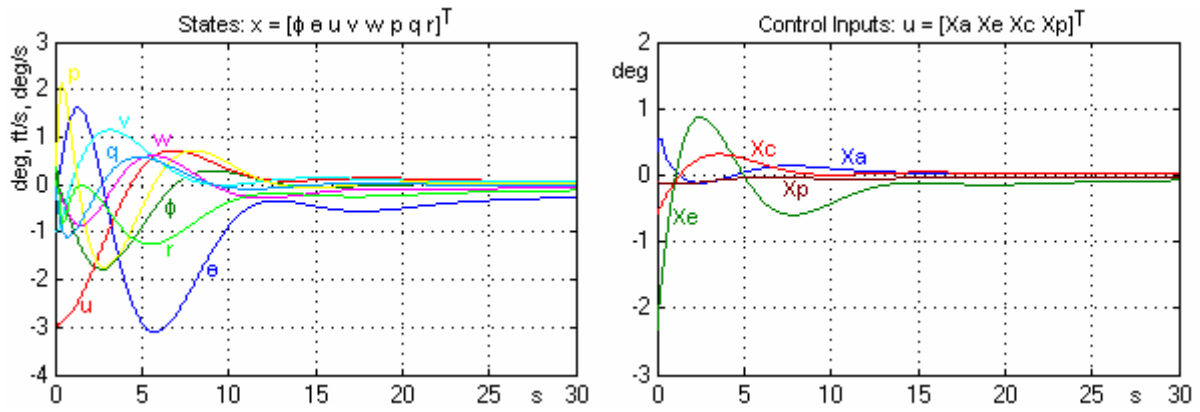


Fig.7 Time responses of states and control inputs in 40kt forward flight at the sea level ($u = -3\text{ft/s}$, $v = -1\text{ ft/s}$)

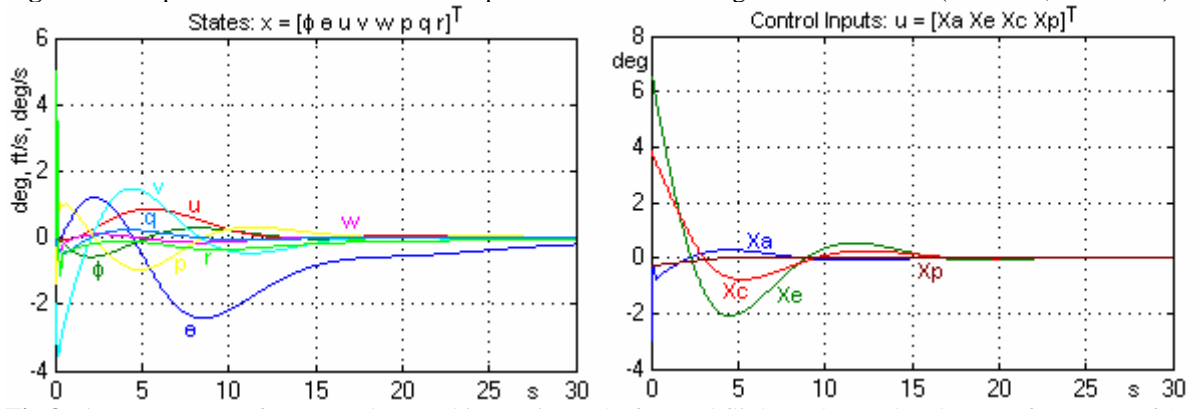


Fig.8 Time responses of states and control inputs in 100kt forward flight at the sea level ($v = -2\text{ft/s}$, $w = -1\text{ ft/s}$)